

# Heat Transfer in a Non-Newtonian Fluid Past a Horizontal Circular Cylinder in Non-Darcy Porous Medium with Suction\Injection Effects

L. Nagaraja<sup>1,2</sup>, M. Sudhakar Reddy<sup>1\*</sup> and M. Surya Narayana Reddy<sup>2</sup>

<sup>1</sup>Department of Mathematics, Madanapalle Institute of Technology & Science, Madanapalle – 517325, Andhra Pradesh, India; msreddy.hod@gmail.com

<sup>2</sup>Department of Mathematics, JNTUA College of Engineering, Pulivendula – 516390, Andhra Pradesh, India

## Abstract

This paper investigates the effects of heat transfer in the convective flow of an Eyring-Powell fluid over a circular cylinder with convective boundary conditions. Consideration of suction and injection effects. Inclined applied magnetic field is taken. Incoming nonlinear modeled problems consume computed for the convergent solutions of velocity and temperature by Finite Difference Keller-Box scheme. Parameters highlighting for velocity and temperature are graphically discussed. Numerical values of skin friction and Nusselt number are also presented in the tabular form.

**Keywords:** Circular Cylinder, Eyring-Powell Fluid, Heat Transfer, MHD, Porous Medium

## NOMENCLATURE

$C_f$	skin friction coefficient
$f$	non-dimensional steam function
$Gr$	Grash of number
$g$	acceleration due to gravity
$k$	thermal conductivity of fluid
$Nu$	local Nusselt number
$Pr$	prandtl number
$f_w$	suction/injection parameter
$T$	temperature of the fluid
$u, v$	non-dimensional velocity components along the x- and y- directions, respectively
$V$	velocity vector x stream wise coordinate y transverse coordinate

## GREEK SYMBOLS

$\alpha$	thermal diffusivity
----------	---------------------

$\beta$	fluid parameter
$\delta$	local non-Newtonian parameter
$\eta$	dimensionless radial coordinate
$\mu$	dynamic viscosity
$\nu$	kinematic viscosity
$\theta$	dimensionless temperature
$\rho$	density of non-Newtonian fluid
$\xi$	dimensionless tangential coordinate
$\psi$	dimensionless stream function
$\varepsilon$	fluid parameter

## SUBSCRIPTS

$W$	condition at the wall
$\infty$	free stream condition

## 1. Introduction

The study of stretched flows with chemical reaction has a vital role in several branches of engineering and sci-

\*Author for correspondence

ence. These effects in flow with heat and mass transfer cannot be neglected especially in design of chemical processing equipment, fog formation and dispersion, crops damage due to freezing, food processing etc. Moreover, effectiveness of this kind of flow can be found in different engineering and industrial applications for instance combustion systems, metallurgy, nuclear reactor safety, solar collector and chemical engineering. Several investigators reported their studies by considering chemical reaction effects. For instance, Eyring-Powell<sup>1</sup> is one amongst these non-Newtonian models. This model has special attraction due to the following facts. Firstly, its fundamental relation is stated empirically. Secondly it illustrates Newtonian behavior for both low and high shear rates. This model with heat transfer further plays important part in distinct industrial, natural and geophysical processes which comprise delivery of dampness and temperature over the agricultural fields, thermal insulation, geothermal reservoirs, environmental pollution, underground energy transport and destruction of crops due to cold. Characteristics of magnetohydrodynamic (MHD) in thermally radiative stretchable flow of Powell-Eyring liquid is explored by Hayat et. al<sup>2</sup>. Recently Malik et. al<sup>3</sup> studied mixed convection flow Eyring-Powell fluid. They found that rate of heat transfer decreases for all parameters. Abdul Gaffar et al studied on<sup>4</sup> and discussed Filled presence of Porous Media under the Effect of Radiation and MHD<sup>5-7</sup>.

Hayat et al studied<sup>8</sup> and discussed temperature dependent thermal conductivity is accounted. Boundary layer stream of an Eyring-Powell ideal fluid due to a cylinder investigated Hina et. al<sup>9</sup>. Noreen et. al<sup>10</sup> investigated of magnetic field effects on Eyring-Powell fluid flow towards a stretching sheet thru finite difference method. Chemically-reactive thermo micro polar transport in porous media (Beg et. al<sup>11</sup>), two-phase magneto-convection in porous media (Zueco et. al<sup>12</sup>). Other recent studies employing non-Darcy transport models in the context of chemical process and medical engineering include (Beg et. al<sup>13,14</sup>). Subba Rao and Nagendra<sup>15</sup> investigated thermal radiation effects on Oldroyd-B viscoelastic Nano fluid flow from a stretching sheet in a non-Darcy porous medium. They analyzed behavior of Nano particles on temperature and concentration distributions in detail. Subba Rao et. al<sup>16</sup> discussed the radiation effects in a Casson non-Newtonian fluid with multiple slip conditions in the presence of porous medium. Magneto-hydrodynamics has found ever-increasing applications in modern smart

technologies. The application of magnetic fields (static or alternating) has been shown to manipulate successfully the material characteristics of electro-conductive polymers which are finding new applications in aerospace, offshore and naval industries. Interesting studies in this regard addressing various systems employing magnetic polymers include environmental engineering<sup>17</sup>, thin film fabrication processes<sup>18</sup> and design of shock dissipation systems with magnetic elastomers<sup>19</sup>. Coating applications and energy systems enhancement with smart magnetic polymers have also grown substantially in recent years. In the context of coating applications, it is critical to regulate heat transfer conditions which lead to improved bonding and homogeneity in engineered polymeric surfaces. Many studies have therefore examined the transport phenomena (i.e. coupled heat and momentum transfer) from different geometrical shapes including cones, pipes, disks and truncated bodies and spheres. The spherical geometry is particularly relevant to chemical engineering processes. Investigators have applied a variety of different material models for the coatings and also numerical methods to solve the associated boundary value problems. Bég et. al<sup>20</sup> used the Homotopy Analysis Method (HAM) to analyze flow from a sphere in a porous medium.

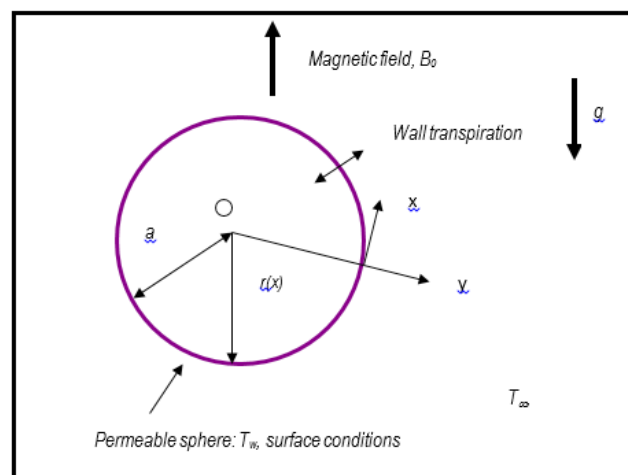


Figure 1: Physical Model and Coordinate System

Trendy the present investigation, we consider the *boundary layer movement of a non-Newtonian Eyring Powell fluid on circular cylinder*. A finite difference numerical solution is obtained for the transformed nonlinear two-point boundary value problem subject to physically suitable boundary circumstances at the cylinder surface. The impact of the emerging thermo physical parameters

are presented graphically and in Tables. Validation with previous Newtonian studies is included. Detailed evaluation of the physics is included. The present problem has to the writers' information not appeared thus far in the technical writings.

## 2. Mathematical Flow Model

Two dimensional, stable, in-compressible boundary layer stream of Eyring-Powell fluid thru a circular cylinder in a porous medium in the occurrence of magnetic field (Figure 1). The boundary layer rough calculation, the leading preservation equalities of Eyring-Powell fluid<sup>1</sup> is given as

$$\frac{\partial u}{\partial x} + \frac{\partial v}{\partial y} = 0 \quad (1)$$

$$\frac{\partial u}{\partial x} + \frac{\partial v}{\partial y} = \left( \nu + \frac{1}{\rho \beta c} \right) \frac{\partial^2 u}{\partial y^2} - \frac{1}{2 \rho \beta c^3} \left( \frac{\partial u}{\partial y} \right)^2 + g \beta (T - T_\infty) \sin \left( \frac{x}{a} \right) - \frac{\sigma B_0^2}{\rho} u - \frac{\nu}{K} u \quad (2)$$

$$\frac{\partial T}{\partial x} u + \frac{\partial T}{\partial y} v = \alpha \frac{\partial^2 T}{\partial y^2} \quad (3)$$

The boundary circumstances be situated set at the circulation and the advantage of the boundary layer system, correspondingly as follows

$$\begin{aligned} \text{As } y = 0 : \quad u = 0, \quad v = 0, \quad T = 0 \\ \text{At } y \rightarrow \infty : \quad u \rightarrow 0, \quad T \rightarrow T_\infty \end{aligned} \quad (4)$$

The stream function  $\psi$  is defined by the Cauchy

$$\text{Riemann equations, } u = \frac{\partial \psi}{\partial y} \text{ and } v = -\frac{\partial \psi}{\partial x}, \text{ and therefore}$$

the continuity equation is automatically satisfied. In command to write the governing equations and the frontier circumstances in dimensionless procedure, the succeeding non-dimensional measures are acquainting with:

$$\begin{aligned} \xi = \frac{x}{a}, \quad \eta = \frac{y}{a} Gr^{1/4}, \quad \psi = \nu \xi Gr^{1/4} f, \quad M = \frac{\sigma B_0^2 a^2}{\rho \nu Gr^{1/2}}, \\ Da = \frac{K}{a^2}, \quad \theta = \frac{T - T_\infty}{T_w - T_\infty}, \quad Gr = \frac{g \beta (T_w - T_\infty) a^3}{\nu^3}, \quad Pr = \frac{\nu}{\alpha} \end{aligned} \quad (5)$$

In view of non-dimensional parameters (5), Calculations (1)-(3) moderate to the succeeding joined, nonlinear, dimensionless differential calculations (partial) are:

$$(1 + \varepsilon) f''' - f'^2 + f f'' - \varepsilon \delta \xi^2 f'^2 f'' - \left( M + \frac{1}{Da Gr^{1/2}} \right) f' + \frac{\sin \xi}{\xi} \theta = \xi \left( f' \frac{\partial f'}{\partial \xi} - f'' \frac{\partial f}{\partial \xi} \right) \quad (6)$$

$$\frac{1}{Pr} \theta'' + f \theta' = \xi \left( f' \frac{\partial \theta}{\partial \xi} - \theta' \frac{\partial f}{\partial \xi} \right) \quad (7)$$

The transformed dimensionless boundary conditions are:

$$\begin{aligned} f = 0, \quad f' = 0, \quad \theta = 1, \quad \text{At } \eta = 0 \\ f' \rightarrow 0, \quad \theta \rightarrow 0, \quad \text{As } \eta \rightarrow \infty \end{aligned} \quad (8)$$

The manufacturing design measures of corporeal attention include the skin-friction factor and Nusselt number, are given by,

$$C_f Gr^{-3/4} = (1 + \varepsilon) \xi f''(0) - \frac{\delta}{3} \varepsilon \xi^3 (f''(\xi, 0))^3 \quad (9)$$

$$\frac{Nu}{\sqrt{Gr}} = -\theta'(0) \quad (10)$$

## 3. Numerical Solutions

The coupled boundary layer equations in a (x,h) coordinate system remain strongly nonlinear. A numerical method, the implicit difference Keller-Box method, is therefore deployed to solve the boundary value problem defined by Ens. (6)-(7) with boundary conditions (8). This procedure has been labeled concisely in Cebeci and Bradshaw<sup>21</sup> and Keller<sup>22</sup>. It has been used recently in polymeric flow dynamics by Subba Rao et. al<sup>23,24</sup> for viscoelastic models.

## 4. Results and Discussion

Table 1. Shows the comparison values of the present study with those obtained by Gaffar et. al<sup>25</sup> found to be in excellent agreement.

The side view for temperature and velocity various values of magnetic parameter (M) as shown in Figure 2(a) and Figure 2(b). It is observed that a decrease in the magnetic parameter (M) suggestively decelerates the stream i.e., velocity declines. Also decreasing magnetic parameter (M) is found to decelerate the temperature. The side view for velocity and temperature for various values of porous medium (E) as shown in Figure 3(a) and Figure 3(b). It is observed that decrease in the porous medium significantly decelerates the flow i.e., velocity decreases. Also increasing porous medium is found to decelerate the temperature. The outline for velocity and temperature for

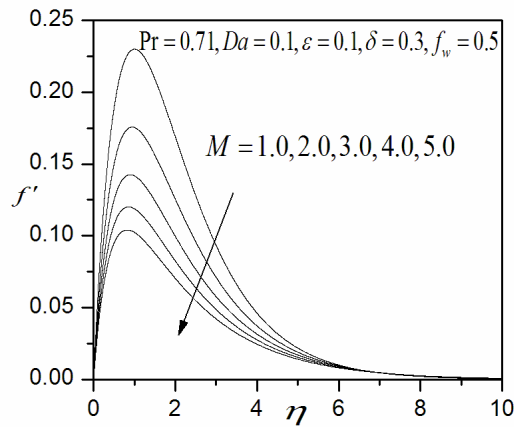


Fig. 2(a). Velocity profiles for different values of  $M$

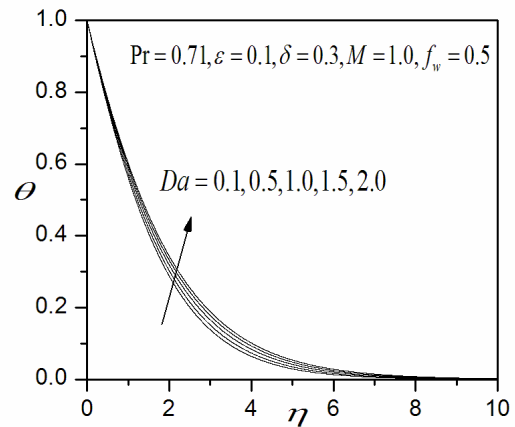


Fig. 3(b). Temperature profiles for different values of  $Da$

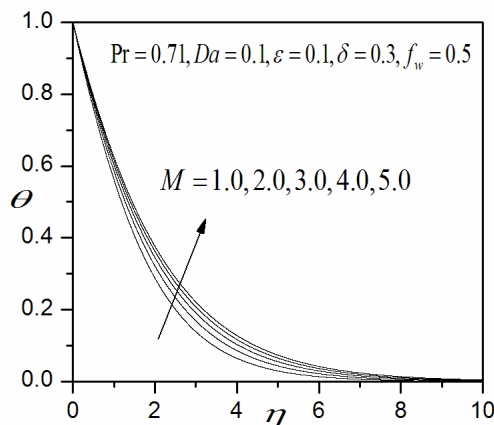


Fig. 2(b). Temperature profiles for different values of  $M$

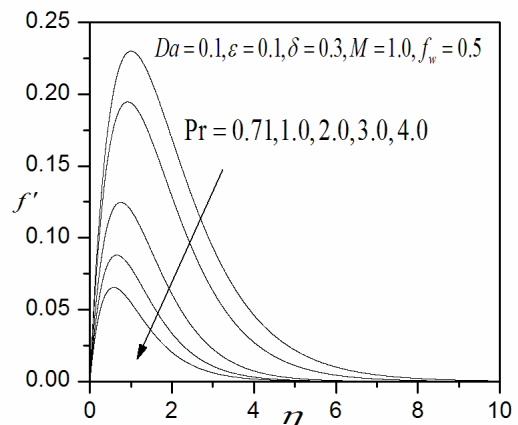


Fig. 4(a). Velocity profiles for different values of  $Pr$

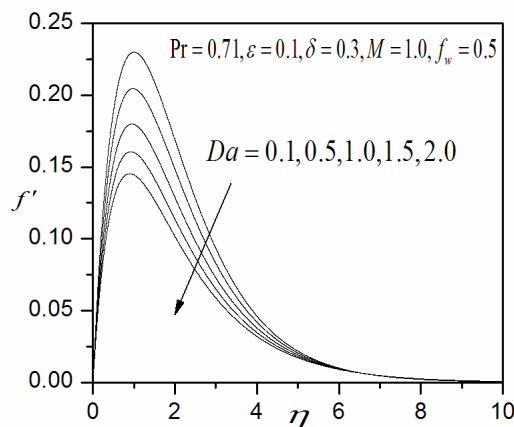


Fig. 3(a). Velocity profiles for different values of  $Da$

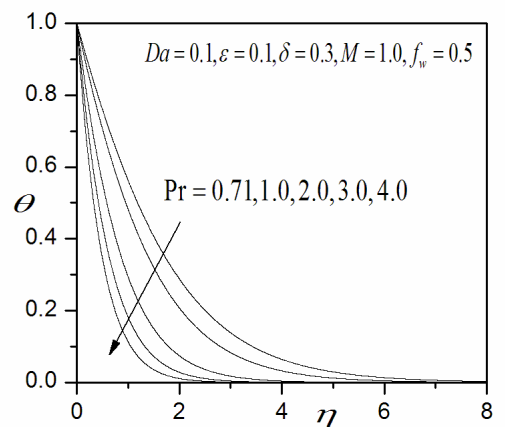
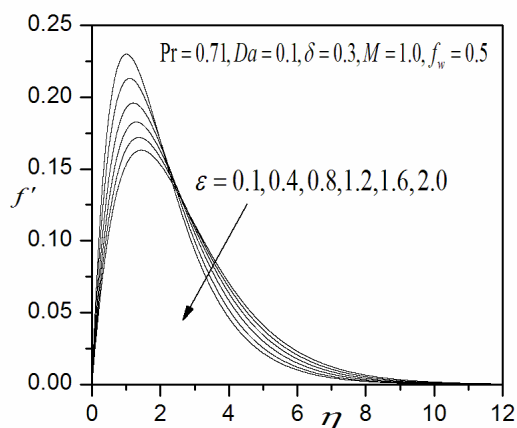
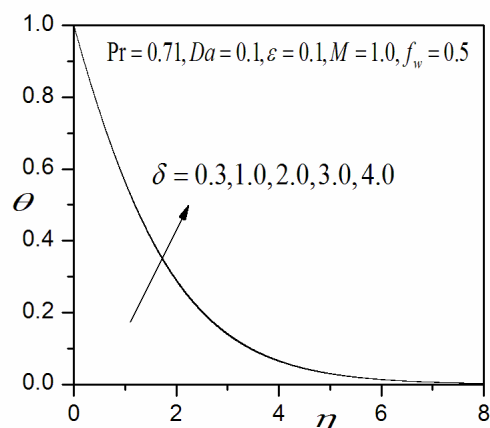
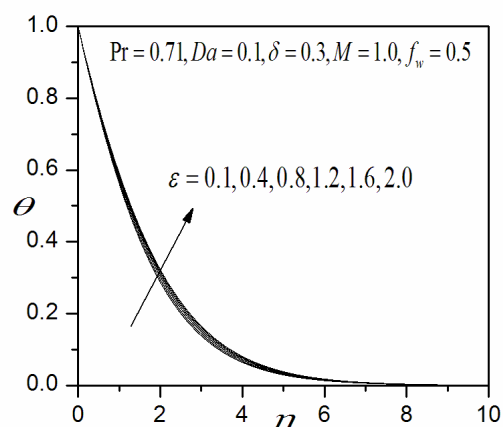
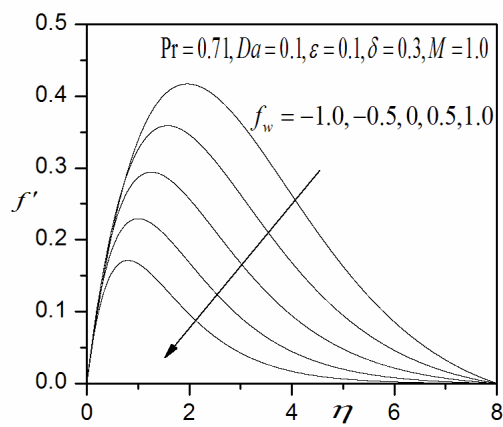
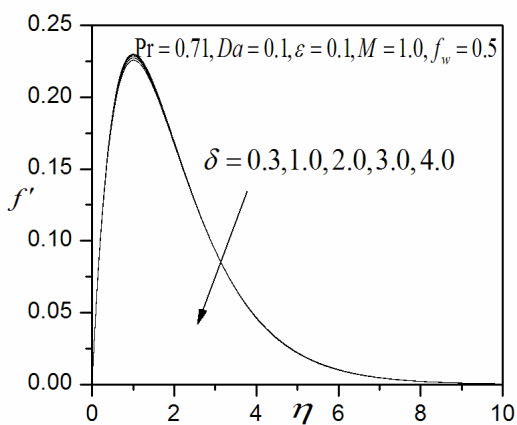
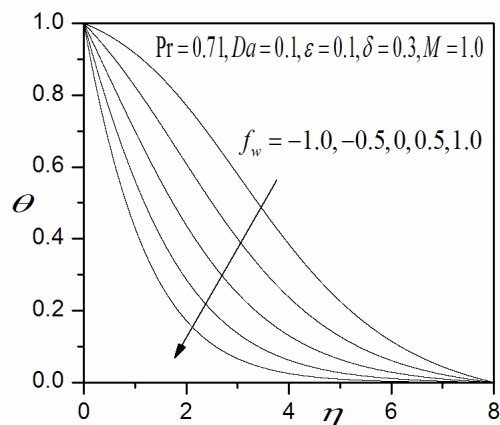


Fig. 4(b). Temperature profiles for different values of  $Pr$


Fig. 5(a). Velocity profiles for different values of  $\varepsilon$ 

Fig. 6(b). Temperature profiles for different values of  $\delta$ 

Fig. 5(b). Temperature profiles for different values of  $\varepsilon$ 

Fig. 7(a). Velocity profiles for different values of  $f_w$ 

Fig. 6(a). Velocity profiles for different values of  $\delta$ 

Fig. 7(b). Temperature profiles for different values of  $f_w$

various values of Prandtl number ( $Pr$ ) as shown Figures 4(a) and 4(b). It is observed that an increase in the Prandtl number significantly decelerates the flow i.e., velocity decreases. Also increasing Prandtl number is found to decelerate the temperature. The effect of Eyring-Powell fluid parameter  $\epsilon$ , on the velocity and temperature allocations through the boundary layer command. Figures 5(a) and 5(b) shows that Velocity is significantly decreased with increasing  $\epsilon$  at larger distance from the cylinder surface owing to the simultaneous drop in dynamic viscosity. The velocity and temperature distribution with increasing local non-Newtonian parameter. Very little tangible effect is observed in Figure 6(a), although there is very slight increase in  $\delta$ . Similarly, there is only a very slight depression in temperature magnitude in Figure 6(b) with rise in  $\delta$ . Figures 7(a) and 7(b) depicts the influence of suction/blowing on the velocity and temperature profiles. The positive values (suction,  $f_w' > 0$ ) for the flow of the fluid and temperature are decelerated. Conversely with increased blowing i.e. injection of fluid via the cylinder surface in to the porous medium regime, ( $f_w' < 0$ ), the flow is strongly accelerated i.e. velocities are increased. As anticipated the case of a solid cylinder ( $f_w' = 0$ ) falls between the weak suction and weak blowing cases.

**Table 1.** Comparison table of  $f''(\xi, 0)$  and  $-\theta'(\xi, 0)$  for different values of  $\xi$

$\xi$	Gaffar et. al <sup>25</sup>		Present	
	$f''(\xi, 0)$	$-\theta'(\xi, 0)$	$f''(\xi, 0)$	$-\theta'(\xi, 0)$
0.1	0.0653	6.4626	0.0659	6.4627
0.2	0.1313	3.4924	0.1311	3.4920
0.4	0.2644	2.0225	0.2645	2.0219
0.6	0.3960	1.5436	0.3952	1.5431
0.8	0.5232	1.3243	0.5235	1.3239
1.0	0.6427	1.1992	0.6431	1.1988
1.5	0.8872	1.0571	0.8872	1.8862

## 5. Conclusion

Numerical solutions consume presented for heat transfer of Eyring-Powell flow through a cylinder. Keller-box accurate structure has been employed to resolve the altered equation, dimensionless velocity and boundary layer calculations, subject to realistic circumstances. Excellent correlation with previous studies has been dem-

onstrated testifying to the validity of the present code. The conclusions have here:

1. Increasing Eyring-Powell fluid parameter ( $\epsilon$ ), decline the velocity and skin friction, rate of heat transfer, whereas it lift up temperatures in the boundary layer.
2. Increasing local non-Newtonian parameter ( $\delta$ ), the velocity, skin friction and Nusselt number growths for all values of tangential coordinate( $\xi$ ) i.e., during the boundary layer regime while it low temperature.

## 6. References

1. Powell RE, Eyring H. Mechanisms for the relaxation theory of viscosity. *Nature*. 1944; 154:427–8. Crossref
2. Hayat T, Awais M, Asghar S. Radiative effects in three-dimensional flow of MHD Eyring-Powell fluid. *Journal of the Egyptian Mathematical Society*. 2013; 21:379–84. Crossref
3. Malik MY, Khan I, Hussain A, Salahuddin T. Mixed convection flow of MHD Eyring-Powell nano fluid over a stretching sheet a numerical study. *AIP advances*. 2015; 5:117–18. Crossref
4. Gaffar SA, Prasad R, Reddy EK. Computational study of non-Newtonian Eyring-powell fluid from a horizontal circular cylinder with biot number effects. *International Journal of Mathematical Archive*. 2015; 6(9):114–32.
5. Mohammed H, AL-Hafidh MH, Jubair HK. Comparison between two vertical enclosures filled with porous media under the effect of radiation and magneto hydrodynamics. *Journal of Energy and Power Engineering*. 2013; 7:37–49.
6. Qing J, Bhatti MM, Abbas MA, Rashidi MM, Ali ME. Entropy generation on mhd casson nano fluid flow over a porous stretching/shrinking surface. *Entropy*. 2016; 18(4):123.
7. Hakeem AKA, Ganesh NV; Ganga B. Heat transfer of non-Darcy MHD flow of nano-fluid over a stretching/shrinking surface in a thermally stratified medium with second order slip model. *Scientia Iranica*. 2015; 22(6):2766–84.
8. Waqas M, Khan MI, Hayat T, Alsaedi A, Khan MI. On Cattaneo-Christov heat flux impact for temperature-dependent conductivity of Powell-Eyring liquid. (In press). 2017. Crossref
9. Hina S, Mustafa M, Hayat T, Alsaedi A. Peristaltic transport of Powell-Eyring fluid in a curved channel with heat/mass transfer and wall properties. *International Journal of Heat and Mass Transfer*. 2016; 101:156–65. Crossref
10. Akbar NS, Ebaid AH, Khan ZH. Numerical analysis of magnetic field effects on Eyring-Powell fluid flow towards a stretching sheet. *Journal of Magnetism and Magnetic Materials*. 2015; 382:355–8. Crossref



11. Bég OA, Bhargava R, Rawat S, Takhar HS, Bég TA. A study of buoyancy driven dissipative micropolar free convection heat and mass transfer in a Darcian porous medium with chemical reaction. *Nonlinear Analysis: Modeling and Control*. 2007; 12:157–80.
12. Zueco J, Bég OA. Network simulation solutions for laminar radiating dissipative magneto-gas dynamic heat transfer over a wedge in non-Darcian porous regime. *Mathematical and Computer Modelling*. 2009; 50:439–52. Crossref
13. Bég OA, Makinde OD, Zueco J, Ghosh SK. Hydromagnetic viscous flow in a rotating annular high-porosity medium with nonlinear Forchheimer drag effects: numerical study. *World Journal of Modelling and Simulation*. 2012; 8:83–95.
14. Bég OA. Numerical methods for multi-physical magneto hydrodynamics. Ch. 1, *New Developments in Hydrodynamics Research*, Ibragimov MJ, Anisimov MA, editors. Nova Science, New York; 2012b. p. 1–110.
15. Rao AS, Nagendra N. Thermal radiation effects on Oldroyd-B Nano fluid from a stretching sheet in a non-Darcy porous medium. *Global Journal of Pure and Applied Mathematics*. 2015; 11:45–9.
16. Rao AS, Prasad VR, Harshavall K, Bég OA. Thermal radiation effects on non-Newtonian fluid in a variable porosity regime with partial slip. *Journal of Porous Media*. 2016; 19(4):313–29, <http://dx.doi.org/10.1615/JPorMedia.v19.i4.30> Crossref
17. Rojas JA, Santos K. Magnetic nanophases of iron oxide embedded in polymer. Effects of magneto-hydrodynamic treatment of pure and wastewater. 5th Latin American Congress on Biomedical Engineering CLAIB; 2011 May 16–21, Habana, Cuba; 2011.
18. Yonemura H, Takata M, Yamada, S. Magnetic field effects on photoelectrochemical reactions of electrodes modified with thin films consisting of conductive polymers. *Journal of Applied Physics*. 2014; 53:01AD06. Crossref
19. Stepanov GV, Abramchuk SS, Grishin DA, Nikitin LV, Kramarenko E, Khokhlov AR. Effect of a homogeneous magnetic field on the viscoelastic behavior of magnetic elastomers. *Polymer*. 2007; 48:488–95. Crossref
20. Bég TA, Bég OA, Rashidi MM, Asadi M. Homotopy semi-numerical modelling of nanofluid convection flow from an isothermal spherical body in a permeable regime. *International Journal of Microscale and Nanoscale Thermal and Fluid*. 2012; 3:237–66.
21. Cebeci T, Bradshaw P. 1984 *Physical and computational aspects of convective heat transfer*. Springer, New York. Crossref
22. Keller HB. A new difference method for parabolic problems, Bramble J, editor. *Numerical Methods for Partial Differential Equations*, Academic Press, New York, USA; 1970.
23. Rao AS, Prasad VR, Nagendra N, Murthy KVN, Reddy NB, Bég OA. Numerical Modeling of Non-Similar Mixed Convection Heat Transfer over a Stretching Surface with Slip Conditions, *World Journal of Mechanics*. 2015; 5:117–28.
24. Prasad VR, Rao AS, Bég OA. Flow and heat transfer of casson fluid from a horizontal circular cylinder with partial slip in non-darcy porous medium. *Journal of Applied & Computational Mathematics*. 2013; 2:3.
25. Gaffar SA, Prasad VR, Vijaya B. Computational study of non Newtonian Eyring–Powell fluid from a vertical porous plate with biot number effects. *Journal of the Brazilian Society of Mechanical Sciences and Engineering*. 2017; 39(7):2747–65. Crossref